Generation of coherent THz Cherenkov radiation by electron bunch tilt control

Yuichi Tadenuma,[1,*] Kazuyuki Sakaue,[1,2,†] Tomohiro Toida,[1] Mariko Nishida,[1] Mari Brameld,[1] Tatsuki Murakami,[1] Ryo Yanagisawa,[1] Masakazu Washio,[1] and Ryunosuke Kuroda[3]

[1]*Research Institute for Science and Engineering, Waseda University, 17 Kikuicho, Shinjuku-ku, Tokyo 162-0044, Japan*
[2]*Photon Science Center, The University of Tokyo, 7-3-1 Hongo, Bunkyo-ku, Tokyo 113-8656, Japan*
[3]*Operando-OIL, National Institute of Advanced Industrial Science and Technology (AIST) 5-1-5 Kashiwano-ha, Kashiwa, Chiba 277-8589, Japan*

(Received 30 July 2022; accepted 4 November 2022; published 22 November 2022)

We propose a new method that generates coherent Cherenkov radiation by controlling the tilt of the electron bunch. In this scheme, the wavelength band of coherent radiation depends on the transverse size of the electron bunch. This study demonstrates a coherent Cherenkov radiation (CChR) pulse in the THz region corresponding to the beam size. To generate the CChR, we used a 4.8-MeV electron bunch from a photocathode radio-frequency (rf) gun and controlled the angle through an rf transverse deflecting cavity. Our new method increased the pulse intensity by a factor of 7.3 compared to the case without tilting and the THz pulse characteristics well agreed with the prediction.

DOI: 10.1103/PhysRevAccelBeams.25.110102

I. INTRODUCTION

The intensity of the radiation from relativistic electrons produced by an accelerator strongly depends on the phase overlap of the radiation from each electron. When each contribution has the same phase, the radiation is called *coherent radiation* (CR). As is widely known, the intensities of incoherent radiation (ICR) and CR are proportional to the number and squared number of the electrons in the bunch, respectively. CR was first observed as coherent synchrotron radiation in the submillimeter to millimeter wavelength range when a short electron bunch was generated by a linear accelerator at Tohoku University in 1989 [1]. CR has since been observed in synchrotron radiation [2,3], transition radiation [4–6], diffraction radiation [7,8], Cherenkov radiation [9,10], and Smith-Purcell radiation [11,12]. Because CR beneficially increases the radiation intensity, it has been widely studied in accelerator physics and radiation research. CR is commonly utilized by a free-electron laser, which can now emit wavelengths in the x-ray region [13–15]. The strong dependence of radiation intensity on CR has also been exploited in beam diagnostics [6,8,16,17]. The exact bunch shape can be obtained by analyzing the CR spectrum because the radiation spectrum from the electron bunch reflects the electron density distribution in the bunch. Coherent synchrotron radiation can significantly increase the radiation intensity, and brilliant synchrotron radiation sources emitting over a wide range of wavelengths (infrared to x rays) have now been developed in storage rings and free-electron lasers [18–20]. CR is usually generated by sufficiently shortening the bunch length relative to the radiation wavelength. The present study proposes a method that generates coherent Cherenkov radiation (CChR) using tilt control of the electron bunch rather than bunch compression. To satisfy the phase-matching condition of radiation, the angle of the electron bunch is precisely controlled to match the Cherenkov radiation angle, which depends on the velocity of the particle and the refractive index of the target medium. In this method, CR is obtained not over the bunch length but over the transverse size of electron bunches. Therefore, CR can be generated whenever the electron beam can be sufficiently focused. In [21] and [22], the authors reported an experimental demonstration of CChR using a tilted electron beam and its dependence on the electron bunch charge and tilt angle, the time waveform, and its Fourier transform. We investigated this method in more detail, such as absolute powers, spot profile, and polarization state, to study the principle of this scheme and clarify its usefulness in achieving CR. We also verified our method by comparing it with theoretical calculations. The resulting THz pulse can generate intense terahertz electric fields. This paper

*yt4869@ruri.waseda.jp
†ksakaue@psc.t.u-tokyo.ac.jp

reports the principle and experimental results of CChR produced by controlling the tilt of the electron bunch with a photocathode radio-frequency (rf) gun and an rf transverse deflecting cavity.

II. COHERENT CHERENKOV RADIATION FROM A TILTED ELECTRON BEAM

To increase the intensity of the radiation from an electron bunch, we must match the phases of the radiation from each electron in the bunch. The radiation intensity from an N-electron bunch can be expressed as

$$P = N[1 + (N-1)f(\lambda)]P_0, \tag{1}$$

where P is the total radiant intensity, P_0 is the radiation intensity from a single electron, and $f(\lambda)$ is a parameter called the *form factor* [23]. In the completely coherent state, $f(\lambda) = 1$ and in the completely incoherent state, $f(\lambda) = 0$. The incoherence and coherence limits of Eq. (1) are given by

$$P = \begin{cases} NP_0 & \text{(incoherence limit)}, \\ N^2P_0 & \text{(coherence limit)}. \end{cases} \tag{2}$$

As an actual electron bunch has a finite length, it never reaches the limit in Eq. (2); instead, it emits a mixture of CR and ICR. Therefore, the radiation intensity of a real electron bunch is

$$P = NP_0 + N_c^2P_0, \tag{3}$$

where the first and second terms are contributed by ICR and CR, respectively. $N_c = Nf(\lambda)$, defining the number of electrons contributing to CR, is usually increased by sufficiently compressing the bunch length relative to the radiation wavelength. Bunch compression methods include energy chirp in bunches [24] and velocity difference in bunches [25,26]. In the relatively low-energy region, the space-charge effect limits the number of electrons or the achievement of sufficient bunch compression. The generation of ultrashort electron bunches of a few MeV has only been successful with an electron beam charge of a few pC at most because of the space-charge effects. [27].

Cherenkov radiation is a shock wavelike radiation produced when a charged particle moves through a dielectric with a velocity exceeding the phase velocity of light in the medium. As shown in Fig. 1, Cherenkov radiation forms a conical radiation wavefront that moves at an angle depending on the velocity of the particle and the refractive index of the medium. The radiation angle θ_c is calculated as

$$\cos\theta_c = \frac{1}{\beta n}, \tag{4}$$

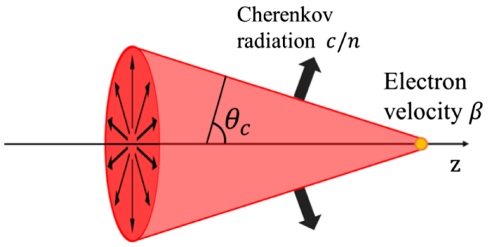

FIG. 1. Diagram of Cherenkov radiation. When a charged particle travels with a velocity β exceeding the velocity of light in a medium c/n, Cherenkov radiation is generated in the form of a cone with the particle's orbit as its axis.

where n is the refractive index of the medium and $\beta = v/c$ is the ratio of the electron velocity v to the light velocity in vacuum c. The radiation is radially polarized along the axis of electron propagation [28].

To generate CChR, we proposed tilt control of the bunch. As Cherenkov radiation is generated at the angle given by Eq. (4), the wavefronts emitted at each point do not overlap while the electron bunch propagates through the medium. However, including the tilt angle of the bunch as a new parameter introduces an additional degree of freedom to the electron bunch. If the electron bunch is injected into the target medium at a precisely controlled tilt angle ψ corresponding to the Cherenkov angle (see Fig. 2), the radiation generated from any position in the electron bunch can be overlapped with the same phase. This phase-matching method is possible because the electron bunch moves at velocity $\beta \sim 1$, whereas the phase velocity of light through the medium is c/n. This principle is equivalent to velocity matching by pulse-front tilting of a laser [29]. In this method, the beam size rather than the bunch length

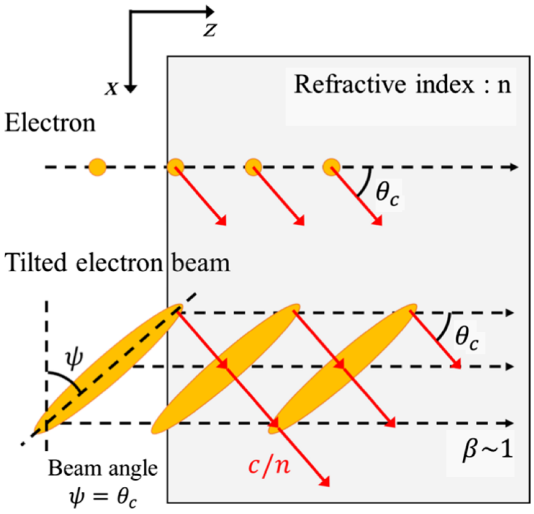

FIG. 2. Phase-matching principle using the tilted electron beam. The Cherenkov radiation generated at each point of the electron beam trajectory can be overlapped by matching the Cherenkov angle with the electron beam tilt angle.

contributes to the form factor in CR, so CR is easily obtained by focusing the electron beam.

To evaluate the principle of CChR with tilted electron beams, we performed a numerical analysis using simulation codes and theoretical formulas. The calculations were mainly based on the penetration depth of an electron through the medium, the form factor of the tilted electron beam, and the theoretical equation of Cherenkov radiation. EGS5, a general Monte Carlo simulation package, was used to calculate the penetration depth and scattering of 4.8-MeV electrons in TOPAS. Regarding the form factor of a tilted electron beam, CChR from asymmetric 3D Gaussian bunches has been already reported in detail in Ref. [30], and we have performed numerical calculations using the following equation based on their Eq. (18) in Ref. [30],

$$f(\omega,\psi) = e^{-\frac{1}{2}(k_x\sigma_x)^2} e^{-\frac{1}{2}[k_y\sin(\psi)+q_z\cos(\psi)]^2\sigma_y^2} \times e^{-\frac{1}{2}[q_z\sin(\psi)-k_y\cos(\psi)]^2\sigma_z^2},$$
$$\text{where } \{k_x,k_y,q_z\} = \frac{\omega}{c}\{\sin(\theta)\sin(\phi),\sin(\theta)\cos(\phi),1/\beta\}. \quad (5)$$

In Eq. (5), ω is the frequency of radiation, σ_x, σ_y are the beam sizes, σ_z is the bunch length, and θ, ϕ are the polar and azimuthal angles. Based on Eq. (5), we obtained the form factor of the tilted electron beam by specifying the electron beam parameters and the observation angle. According to Eq. (5), the point of the beam tilt control scheme is that the form factor is less sensitive to the bunch length than the beam size on the horizontal axis when the bunch is tilted on the x-z plane (our experimental setup). Therefore, this scheme does not require the 3D-focused beam but rather a transverse-focused and tilt-controlled bunch for CChR generation. The relaxation of the requirement to eliminate the need for one-dimensional focusing is a significant advantage for low-energy electron beams, where space-charge effects are strong. We used the classical Frank-Tamm radiation intensity equation to calculate the number of photons N_{photon} of Cherenkov radiation from a single electron as follows:

$$N_{\text{photon}} = 2\pi\alpha l\left(\frac{1}{\lambda_2}-\frac{1}{\lambda_1}\right)\left(1-\frac{1}{\beta^2 n^2}\right), \quad (6)$$

where α is the fine structure constant, l is the penetration depth, indicating the number of photons emitted by an electron within the spectral region between the wavelengths λ_1 and λ_2 [28].

III. EXPERIMENTAL SETUPS

The experimental setup and parameters of the electron beam are shown in Fig. 3 and Table I, respectively. The electron source is an S-band, 1.6-cell photocathode rf electron gun [31], and the electrons produced from the Cs-Te photocathode are accelerated to 4.8 MeV. The electron beam is focused at the target position by two quadrupole magnets. A transverse deflecting cavity installed after the quadrupole magnet controls the tilt angle of the electron beam. The rf transverse deflecting cavity is another S-band, two-cell cavity operated in TM210 mode [32,33]. The tilt angle can be precisely controlled by adjusting the electromagnetic field in the cavity with an rf attenuator. The phase of the electromagnetic field is controlled by a phase shifter, which corresponds to the center position in the horizontal direction of the electron bunch. The deflecting cavity provides transverse forces correlated with the longitudinal electron position and converts it to the positional tilt, after traveling some distance, and the drift length in this experiment is 0.46 m. The charge in the electron bunch is measured by a fast current transformer installed after the deflecting cavity. Finally, the beam position is shifted to the center of the target medium using a steering magnet.

The expected upper-limit frequency of CChR is several THz because the beam size is approximately 250 μm (Table I). The CChR generated from the tilted electron

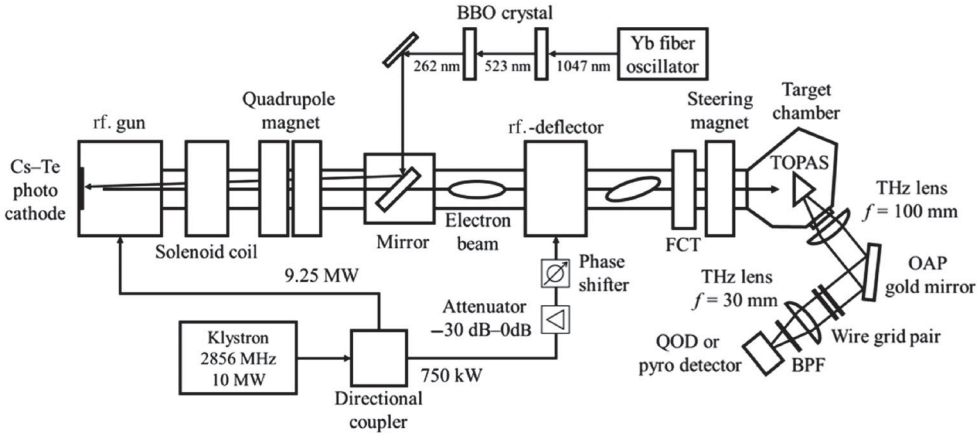

FIG. 3. Experimental setup.

TABLE I. Typical parameters of the electron beam.

Energy [MeV]	4.8
Repetition rate [Hz]	5
Beam size (rms) [μm]	255
Bunch length (rms) [ps]	2.5

beam is extracted through a z-cut crystal quartz window and transported to a detector through two THz lenses and a gold-coated planar mirror. Several types of THz detectors were employed in the present experiment. For first radiation detection and beam-parameter optimization, we employed a quasioptical detector (QOD, Virginia Diodes, Inc.), which combines a Schottky diode and a Si lens and detects a wide range of THz frequencies (0.1–1.0 THz) with high sensitivity and high speed [34]. A pyroelectric device (PYD-1, PHLUXi, Inc.), a heat-sensing power meter (3A-P-THz, Ophir Optronics), and a terahertz camera (IRV-T0831, NEC) were used as required by the objectives of each measurement. To detect specific frequencies, we installed THz bandpass filters (TYDEX) with an approximate bandwidth of 10%.

As the target medium for generating Cherenkov radiation, we trialed high-resistivity silicon ($n = 3.42$) [35], TOPAS ($n = 1.53$) [36], and silica aerogel ($n = 1.03$) [37]. A medium with a high refractive index produces a large number of photons of Cherenkov radiation per unit length, but its high density prevents the deep penetration of electrons. In both the Si and aerogel media, the intensity of the THz pulse was below the detection limit of the power meter. We considered that the Si medium was too dense for sufficient CChR generation by 5-MeV electrons, whereas the silica aerogel had a low refractive index that suppressed the intensity per unit length. As the properties of TOPAS were between those of the other media, TOPAS provided both sufficient intensity per unit length and deep penetration. Therefore, all experimental results in this paper were obtained in TOPAS, an amorphous cyclic olefin copolymer made by copolymerizing norbornene and ethylene over a metallocene catalyst. TOPAS has a low absorption coefficient, and the refractive index is almost constant at 1.53 in the THz spectral region (0.1–1.0 THz) [36]. These characteristics enable phase-matching condition over a wide frequency range. At a refractive index of 1.53, the Cherenkov radiation angle is $\theta_c = 49.2°$. The TOPAS medium was designed as an isosceles triangular prism with the Cherenkov angle. The generated THz pulses could then be extracted perpendicularly from the medium surface. The target was 14 mm wide in the incident plane of the electron bunch, 11 mm wide in the output plane of the CChR pulse, and 10 mm high.

IV. RESULTS

We first measured the beam angle dependence of the CChR pulse intensity by changing the phase and intensity of the electromagnetic field in the rf transverse deflecting cavity. The measurements were performed with a bandpass filter (BPF) with a center frequency of 0.3 THz. The charge per electron bunch was adjusted to 100 pC. Panels (a) and (b) of Fig. 4 show the results of tilting in the correct direction (Fig. 2) and the opposite direction (obtained by changing the rf phase of the deflecting cavity by 180°), respectively. The shift amount was controlled by the attenuator. By increasing the deflection voltage, the shift was enlarged to obtain the shape of the graphs shown in Fig. 4. The pulse intensity was maximized at an approximate bunch angle of 49°, which almost equals the Cherenkov angle (49.2°). The THz intensity was much smaller in the opposite tilt direction [Fig. 4(b)] than that at the correct angle. At maximum, the intensity in the correct direction was more than threefold in the opposing direction. A comparison of calculated and measured beam tilt angle dependence is shown in Fig. 5. The measured values shown in Fig. 5 are the average of six data around the beam shift = 0 mm of each angle taken from Fig. 4(a). The electron beam tilt angle dependence on CChR intensity agreed well with the theoretical prediction. The dependence of the CChR intensity on the tilt angle in this scheme is only a

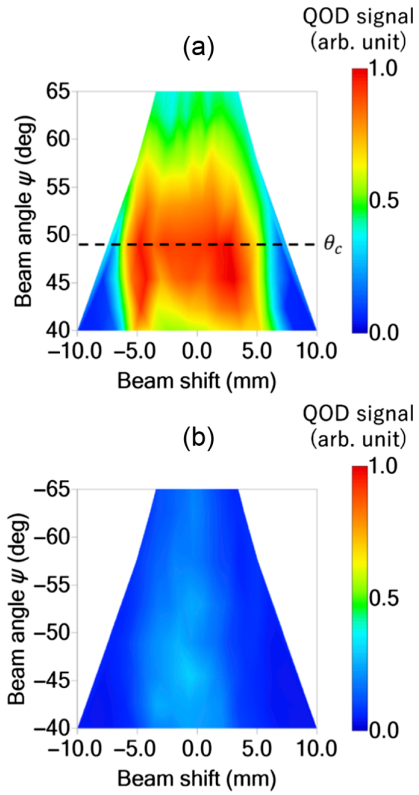

FIG. 4. THz intensities on the tilt angle versus beam shift plane. The QOD signal, indicated by the color bar, represents the THz intensity measured by the QOD, which is normalized by the maximum value. The signal intensity increased at the Cherenkov radiation angle (a) but did not change at the reverse angle (b). The beam shift on the horizontal axis refers to the shift of the electron bunch position.

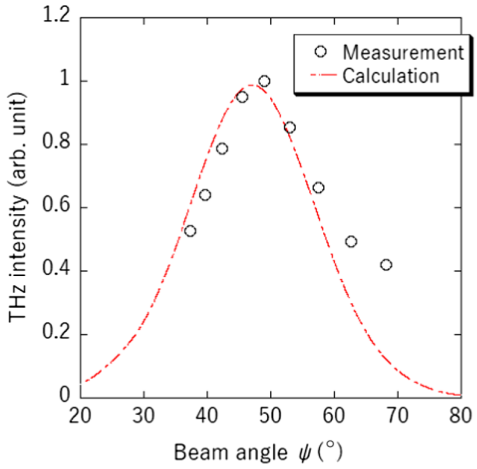

FIG. 5. Comparison of calculated and measured values in the relationship between beam angle and THz intensity. The measured values are the average of six data around the beam shift = 0 mm of each angle taken from Fig. 4(a).

10% decrease in intensity even at ±5° tilt angle, indicating that the method is robust and has a relatively large tolerance in the beam angle.

Figure 6 plots the CChR pulse intensity versus charge in the electron bunch for different values of the tilt angle ψ. Each line represents a fitting using a quadratic polynomial. The detector was a pyrodetector and no BPF was used. The increase in THz pulse intensity with increasing charge was much larger at $\psi = 49.2°$ than at $\psi = 90°$ and $-49.2°$, indicating that more electrons contributed to the CR at the correct tilting angle than at other angles. At the appropriate tilt angle, the number of electrons contributing to the CR was 2.7 times higher than at $-49.2°$, as calculated from the ratio of radiation intensities at $\psi = 49.2°$ and $-49.2°$. These results confirm that our proposed scheme increases the number of electrons contributing to CR.

We then measured the focusing characteristic of the CChR pulses using the THz camera. Figure 7 shows the

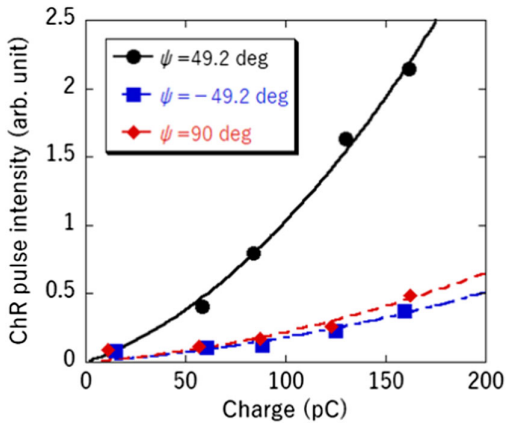

FIG. 6. THz intensity versus charge at various tilt angles. The THz intensity increases proportionally to the square of the charge at $\psi = 49.2°$ and to the charge itself at $\Psi = 49.2°$ and 90°.

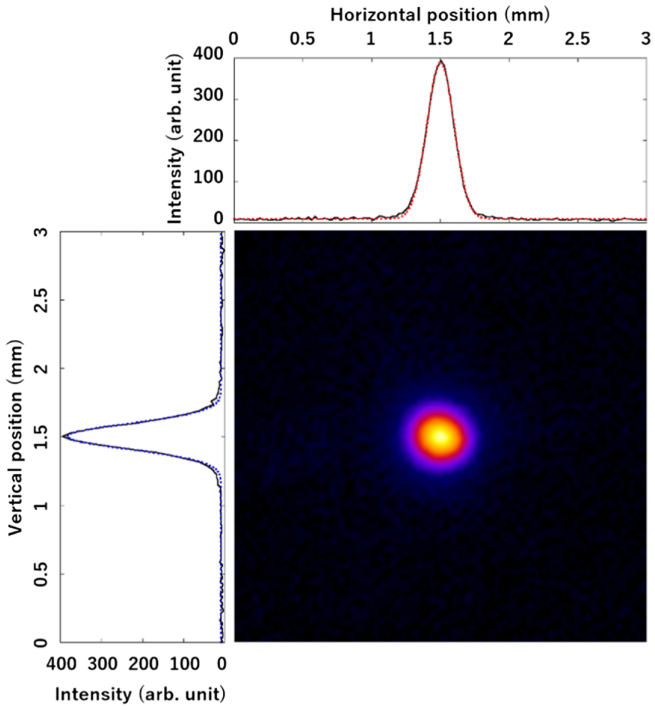

FIG. 7. Spot image of the CChR pulse at the focal point captured using a Terahertz camera. Solid and dotted lines are the measured and Gaussian-fitted values, respectively.

beam spot of the THz pulse after focusing through a THz lens with a focal length of $f = 30$ mm. The horizontal and vertical sizes were 98.2 (rms) and 93.0 μm (rms), respectively, close to the diffraction limit of 96 μm (rms) at 1 THz. The THz camera used in this study is more sensitive at higher frequencies than at lower frequencies and the pulse has a broadband spectrum of over 1 THz. For these reasons, the obtained spot mainly consisted of the higher-frequency part of the THz pulse. The focused spot of the THz pulse indicates that the CChR pulse was well focused in both the horizontal and vertical directions. This small-spot and short-pulse THz pulse will be utilized in applications requiring high fluence, high peak intensity, and a strong electric field.

To measure the polarization characteristics of the pulse, we set up a wire grid polarizer in front of the THz camera. As shown in Fig. 1, the wavefront of the Cherenkov radiation extended conically and was radially polarized around the orbit of an electron. As the phases were matched only in the x-z plane (see Fig. 2), the polarization was expected to be almost linear in the plane formed by the electron orbit and the observation point. Figure 8 plots the THz intensity measured by the THz camera as a function of the angle of the wire grid polarizer. Here the THz intensity is the integration of the intensities in each pixel of the camera. The data were well fitted to the square of the cosine function. From the fitting results and assuming that the detected light contains only linear and unpolarized components, the degree of polarization was calculated as

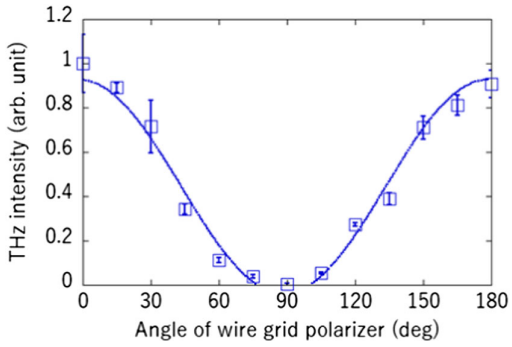

FIG. 8. Polarization characteristic of the CChR pulse measured using a wire grid pair and a THz camera. The solid curve is the best-fitted curve to the data. Error bars represent the fluctuation of THz intensity with standard errors statistically processed by five data of THz camera image.

1.02 ± 0.08, indicating almost linear polarization. The above unity value can be attributed to intensity fluctuations of the THz pulse during the measurements but is deemed reasonable because it lies within the statistical error (± 0.08). Consequently, we confirmed that the generated CChR pulse was almost perfectly p-polarized in the plane formed by the electron beam path and the detector, as predicted by our scheme.

Next, the absolute value of the CChR pulse intensity was measured by a power meter with a sensitive range of 0.1–30 THz. As a single THz pulse produces minuscule heat, we operated a 50-bunch beam with a repetition rate of 119 MHz. In addition, a shutter was opened and closed at 2-m intervals to eliminate the effects of environmental temperature. During these measurements, the charge per electron bunch was set to 380 pC to ensure sufficient intensity for the THz power meter. In addition to the total intensity measurements, the narrowband intensities were measured at 0.3 and 0.6 THz after inserting BPFs with the respective center frequencies into the apparatus. The results are shown in Table II. When the BPF is inserted, the THz intensity at $\psi = 90°$ was too small to be measured by the power meter. However, at the appropriate tilt and without the BPF, the pulse intensity was approximately 7.3 times higher than that without tilting. The maximum pulse intensity was 33 nJ/pulse. As the intensity of CR depends on the electron bunch charge, increasing the charge should further increase the intensity.

TABLE II. Absolute values of the intensities of a CChR pulse (calculated and measured with a power meter).

	$\psi = \theta_c$	$\psi = 90°$	Calculation ($\psi = \theta_c$)
Total [nJ]	33 ± 2.6	4.5 ± 1.6	41
0.3 THz [nJ]	11 ± 1.6	…	12
0.6 THz [nJ]	4.0 ± 1.3	…	2.7

The measured absolute intensity of the THz pulse was checked against simulations and theoretical calculations of the pulse intensity. The calculation results and experimental results are listed in Table II. The measured intensity of the 33 nJ/pulse was 20% smaller than the calculated intensity of the 41 nJ/pulse. Considering the measurement errors and transportation loss of THz pulses conveyed to the detector, the measured intensity was consistent with the calculated intensity, indicating that CChR was achieved by tilting the electron bunch. Extrapolating this scheme to higher-energy electron beams, THz intensities of 83 and 180 nJ/pulse are expected at 10 and 40 MeV, respectively.

Finally, the spectrum of the generated CChR pulses was determined from the electric field waveform acquired by the electro-optic (EO) sampling method [38,39], which reproduces the electric field waveform of the THz pulse by measuring the polarization change of the probe light caused by birefringence when the THz pulse impacts the EO crystal. The measurement setup of the EO sampling method is shown in Fig. 9. The probe laser pulse should have a shorter pulse duration than the THz pulse because it is scanned in time. In this study, the probe light was a Yb fiber femtosecond laser with a pulse duration of 190 fs full width at half maximum (FWHM). The EO crystal was a ZnTe crystal with a thickness of 1 mm. In the system using this EO crystal, the frequency sensitivity at 2 THz was 1 order of magnitude smaller than the maximum value, allowing

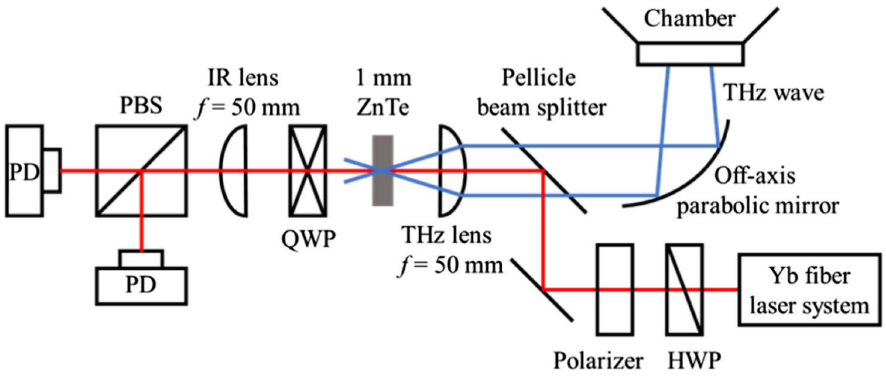

FIG. 9. Schematic of the electro-optic (EO)-sampling measurements. The pellicle beam splitter performs coaxial injection of the coherent Cherenkov radiation pulse (CChR) and the femtosecond laser generated by the Yb fiber laser system into the EO crystal.

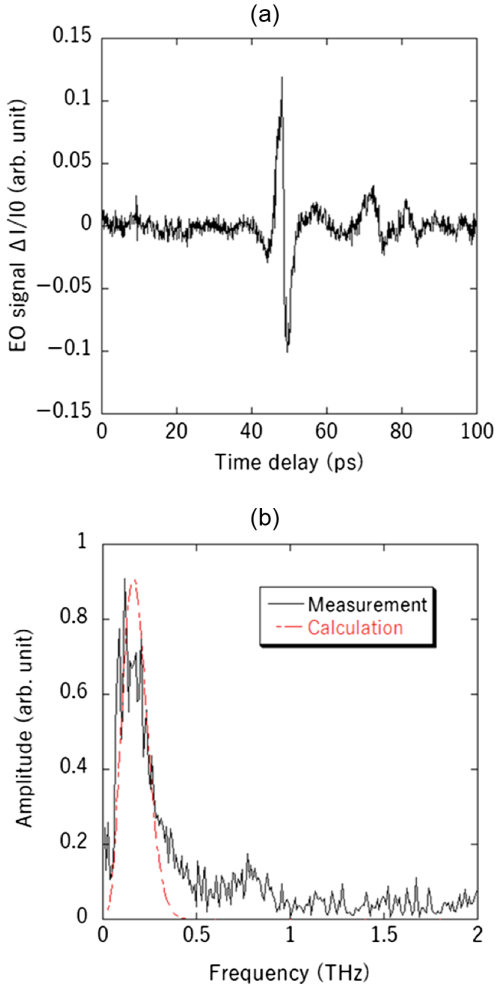

FIG. 10. (a) Electric field waveform of a CChR pulse obtained by EO sampling and (b) its Fourier transform, calculated with a beam size of 400 μm and a bunch length of 2.5 ps.

measurements up to 2 THz. The polarizing beam splitter (PBS) divided the probe laser light transmitted through the ZnTe crystal into p-polarized and s-polarized components, which were separately measured by photodiode detectors (PD). The intensity of both (s- and p-) polarization was adjusted to be equal in the absence of THz pulses. The difference between the signals of the two PDs was determined as the birefringence induced in the EO crystal by the THz pulse. The timing accuracy between the accelerator and the probe laser during accelerator operation was approximately 330 fs rms. The measurement was performed at a high charge (380 pC) to clarify the electric field waveform.

Panels (a) and (b) of Fig. 10 present the measured electric field waveform and its Fourier-transformed spectrum, respectively. As the response to THz waves depends on the type and thickness of the EO crystal, the calculated spectrum reflects the EO response function [40]. The duration of the CChR pulse, calculated by fitting the obtained electric field waveform to a Gaussian function, was 2.5 ps (FWHM). The Fourier transform of the electric field waveform shows a broad spectrum (0.1–1.0 THz), confirming the generation of a broadband and single-cycle THz pulse. The broad peak around 0.8 THz (absent in the calculated spectrum) could be due to the non-Gaussian profile of the electron beam in the experiment, whereas the calculation assumed a Gaussian profile. According to Ref. [41], some electrons that are outside the Gaussian distribution cause a broad spectral spike. The peak power calculated from the THz pulse duration (2.5 ps) and the power meter measurement (33.2 nJ) was 13.3 kW. Furthermore, the maximum electric field strength, which must be high for intense THz pulse applications, was 125 kV/cm when calculated as the focused spot of 100 μm (rms).

V. CONCLUSION

We devised a new method that generates CR in the THz band by phase matching the Cherenkov radiation of multiple sources. The phase matching is achieved by precisely controlling the tilt angle of the electron bunch in an rf transverse deflecting cavity. After adjusting the electron beam angle to the Cherenkov angle, the number of electrons contributing to CR was maximized and the intensity of the CChR pulse was 7.3 times higher than that of the untilted pulse. The generated CChR pulse was well focused and almost perfectly p-polarized, as theoretically predicted. The spectrum measured by EO sampling showed a single cycle and a broadband spectrum of 0.1–1.0 THz, with a maximum peak power exceeding the kW level. All results were consistent with our predictions, demonstrating the generation of CChR via tilt angle control of the electron bunch. The high peak power and a strong focus of the THz pulses generated by this new method ensure a large electric field strength. Therefore, the method is promising for applications requiring high THz electric fields.

In future work, we are planning compact high peak intensity THz pulse generation by accumulating the generated CChR pulses in an optical cavity. The cavity is designed to be a 1.26-m long cavity, corresponding to a bunch-by-bunch interval of 8.4 ns and smaller round trip loss than the CChR generation per bunch. When 100 pulses accumulate in the cavity, the intensity is expected to increase tenfold, further boosting the intensities of the THz pulses.

ACKNOWLEDGMENTS

This work was supported by research grant from The Murata Science Foundation and JSPS KAKENHI 26286083.

[1] T. Nakazato, M. Oyamada, N. Niimura, S. Urasawa, O. Konno, A. Kagaya, R. Kato, T. Kamiyama, Y. Torizuka, T. Nanba, Y. Kondo, Y. Shibata, K. Ishi, T. Ohsaka, and M. Ikezawa, Observation of Coherent Synchrotron Radiation, Phys. Rev. Lett. **63**, 1245 (1989).

[2] K. Ishi, Y. Shibata, T. Takahashi, H. Mishiro, T. Ohsaka, M. Ikezawa, Y. Kondo, T. Nakazato, S. Urasawa, N. Niimura, R. Kato, Y. Shibasaki, and M. Oyamada, Spectrum of coherent synchrotron radiation in the far-infrared region, Phys. Rev. A **43**, 5597 (1991).

[3] M. Abo-Bakr, J. Feikes, K. Holldack, P. Kuske, W. B. Peatman, U. Schade, G. Wüstefeld, and H. W. Hübers, Brilliant, Coherent Far-Infrared (THz) Synchrotron Radiation, Phys. Rev. Lett. **90**, 094801 (2003).

[4] U. Happek, A. J. Sievers, and E. B. Blum, Observation of Coherent Transition Radiation, Phys. Rev. Lett. **67**, 2962 (1991).

[5] T. Takahashi, Y. Shibata, F. Arai, K. Ishi, T. Ohsaka, M. Ikezawa, Y. Kondo, T. Nakazato, S. Urasawa, R. Kato, S. Niwano, and M. Oyamada, Coherent transition radiation at submillimeter and millimeter wavelengths, Phys. Rev. E **48**, 4674 (1993).

[6] Y. Shibata, T. Takahashi, T. Kanai, K. Ishi, M. Ikezawa, J. Ohkuma, S. Okuda, and T. Okada, Diagnostics of an electron beam of a linear accelerator using coherent transition radiation, Phys. Rev. E **50**, 1479 (1994).

[7] Y. Shibata, S. Hasebe, K. Ishi, T. Takahashi, T. Ohsaka, M. Ikezawa, T. Nakazato, M. Oyamada, S. Urasawa, T. Yamakawa, and Y. Kondo, Observation of coherent diffraction radiation from bunched electrons passing through a circular aperture in the millimeter- and submillimeter-wavelength regions, Phys. Rev. E **52**, 6787 (1995).

[8] M. Castellano, V. A. Verzilov, L. Catani, A. Cianchi, G. Orlandi, and M. Geitz, Measurements of coherent diffraction radiation and its application for bunch length diagnostics in particle accelerators, Phys. Rev. E **63**, 056501 (2001).

[9] Y. Shibata, K. Ishi, T. Takahashi, F. Arai, M. Ikezawa, K. Takami, T. Matsuyama, K. Kobayashi, and Y. Fujita, Observation of coherent synchrotron, Čerenkov, and wake-field radiation at millimeter wavelengths using an L-band linear accelerator, Phys. Rev. A **44**, R3449 (1991).

[10] T. Takahashi, T. Kanai, Y. Shibata, K. Ishi, M. Ikezawa, T. Nakazato, M. Oyamada, S. Urasawa, T. Yamakawa, K. Takami, T. Matsuyama, K. Kobayashi, and Y. Fujita, Čerenkov radiation from a finite trajectory of electrons, Phys. Rev. E **50**, 4041 (1994).

[11] K. Ishi, Y. Shibata, T. Takahashi, S. Hasebe, M. Ikezawa, K. Takami, T. Matsuyama, K. Kobayashi, and Y. Fujita, Observation of coherent Smith-Purcell radiation from short-bunched electrons, Phys. Rev. E **51**, R5212 (1995).

[12] S. E. Korbly, A. S. Kesar, J. R. Sirigiri, and R. J. Temkin, Observation of Frequency-Locked Coherent Terahertz Smith-Purcell Radiation, Phys. Rev. Lett. **94**, 054803 (2005).

[13] F. Stephan *et al.*, Detailed characterization of electron sources yielding first demonstration of European X-ray Free-Electron Laser beam quality, Phys. Rev. ST Accel. Beams **13**, 020704 (2010).

[14] C. Bostedt, S. Boutet, D. M. Fritz, Z. Huang, H. J. Lee, H. T. Lemke, A. Robert, W. F. Schlotter, J. J. Turner, and G. J. Williams, Linac coherent light source: The first five years, Rev. Mod. Phys. **88**, 015007 (2016).

[15] I. Inoue, T. Osaka, T. Hara *et al.*, Generation of narrow-band X-ray free-electron laser via reflection self-seeding, Nat. Photonics **13**, 319 (2019).

[16] M. C. Lampel, Coherent Smith-Purcell radiation as a pulse length diagnostic, Nucl. Instrum. Methods Phys. Res., Sect. A **385**, 19 (1997).

[17] S. Casalbuoni, B. Schmidt, P. Schmüser, V. Arsov, and S. Wesch, Ultrabroadband terahertz source and beamline based on coherent transition radiation, Phys. Rev. ST Accel. Beams **12**, 030705 (2009).

[18] M. Abo-Bakr, J. Feikes, K. Holldack, G. Wüstefeld, and H. W. Hübers, Steady-State far-Infrared Coherent Synchrotron Radiation Detected at BESSY II, Phys. Rev. Lett. **88**, 254801 (2002).

[19] P. Emma, K. Bane, M. Cornacchia, Z. Huang, H. Schlarb, G. Stupakov, and D. Walz, Femtosecond and Subfemtosecond X-Ray Pulses from a Self-Amplified Spontaneous-Emission–Based Free-Electron Laser, Phys. Rev. Lett. **92**, 074801 (2004).

[20] C. Bostedt, S. Boutet, D. M. Fritz, Z. Huang, H. J. Lee, H. T. Lemke, A. Robert, W. F. Schlotter, J. J. Turner, and G. J. Williams, Linac coherent light source: The first five years, Rev. Mod. Phys. **88**, 015007 (2016).

[21] K. Sakaue, M. Nishida, M. Washio, R. Kuroda, Y. Taira, and J. Urakawa, Generation of a coherent Cherenkov radiation by using electron bunch tilting, in *Proceedings of the 7th International Particle Accelerator Conference, IPAC-2016, Busan, Korea*, (JACoW, Geneva, Switzerland, 2016), TUPOW047.

[22] K. Sakaue, M. Brameld, M. Nishida, T. Toida, R. Yanagisawa, M. Washio, R. Kuroda, and Y. Taira, Investigation of the coherent Cherenkov radiation using tilted electron bunch, in *Proceedings of the 8th International Particle Accelerator Conference, IPAC'17, Copenhagen, Denmark*, (JACoW, Geneva, Switzerland, 2017), MOPVA024.

[23] T. Takahashi, Y. Shibata, K. Ishi, M. Ikezawa, M. Oyamada, and Y. Kondo, Observation of coherent Čerenkov radiation from a solid dielectric with short bunches of electrons, Phys. Rev. E **62**, 8606 (2000).

[24] B. E. Carlsten and S. J. Russell, Subpicosecond compression of 0.1–1 nC electron bunches with a magnetic chicane at 8 MeV, Phys. Rev. E **53**, R2072 (1996).

[25] S. G. Anderson, P. Musumeci, J. B. Rosenzweig, W. J. Brown, R. J. England, M. Ferrario, J. S. Jacob, M. C. Thompson, G. Travish, A. M. Tremaine, and R. Yoder, Velocity bunching of high-brightness electron beams, Phys. Rev. ST Accel. Beams **8**, 014401 (2005).

[26] K. Sakaue, Y. Koshiba, M. Mizugaki, M. Washio, T. Takatomi, J. Urakawa, and R. Kuroda, Ultrashort electron bunch generation by an energy chirping cell attached rf gun, Phys. Rev. ST Accel. Beams **17**, 023401 (2014).

[27] X. H. Lu, C. X. Tang, R. K. Li, H. To, G. Andonian, and P. Musumeci, Generation and measurement of velocity bunched ultrashort bunch of pC charge, Phys. Rev. ST Accel. Beams **18**, 032802 (2015).

[28] J. V. Jelley, Cerenkov radiation and its applications, Br. J. Appl. Phys. **6**, 227 (1955).

[29] J. Hebling, G. Almási, I. Z. Kozma, and J. Kuhl, Velocity matching by pulse front tilting for large-area THz-pulse generation, Opt. Express **10**, 1161 (2002).

[30] S. Yu. Gogolev and A. P. Potylitsyn, Azimuthal asymmetry of coherent Cherenkov radiation from a tilted bunch, Phys. Lett. A **383**, 888 (2019).

[31] K. Sakaue, H. Hayano, S. Kashiwagi, R. Kuroda, A. Masuda, T. Suzuki, T. Takatomi, N. Terunuma, J. Urakawa, and M. Washio, Cs–Te photocathode RF electron gun for applied research at the Waseda University, Nucl. Instrum. Methods Phys. Res., Sect. B **269**, 2928 (2011).

[32] Y. Nishimura, K. Sakaue, M. Nishiyama, T. Takahashi, M. Washio, T. Takatomi, and J. Urakawa, Design of a two-cell rf-deflector cavity for ultra-short electron bunch measurement, Nucl. Instrum. Methods Phys. Res., Sect. A **764**, 291 (2014).

[33] K. Sakaue, Y. Nishimura, M. Nishiyama, T. Takahashi, M. Washio, T. Takatomi, and J. Urakawa, Temporal profile measurement of an electron bunch with the two-cell rf deflecting cavity at Waseda University, Jpn. J. Appl. Phys. **54**, 026301 (2015).

[34] J. L. Hesler, L. Liu, H. Xu, Y. Duan, and R. M. Weikle, The development of quasi-optical THz detectors, in *Proceedings of 33rd International Conference on Infrared, Millimeter and Terahertz Waves* (2008).

[35] J. Dai, J. Zhang, W. Zhang, and D. Grischkowsky, Terahertz time-domain spectroscopy characterization of the far-infrared absorption and index of refraction of high-resistivity, float-zone silicon, J. Opt. Soc. Am. B **21**, 1379 (2004).

[36] P. D. Cunningham, N. N. Valdes, F. A. Vallejo, L. M. Hayden, B. Polishak, X. H. Zhou, J. Luo, A. K. Y. Jen, J. C. Williams, and R. J. Twieg, Broadband terahertz characterization of the refractive index and absorption of some important polymeric and organic electro-optic materials, J. Appl. Phys. **109**, 043505 (2011).

[37] D. Richter and D. Lipka, Measurement of the refractive index of silica aerogel in vacuum, Nucl. Instrum. Methods Phys. Res., Sect. A **513**, 635 (2003).

[38] C. Winnewisser, P. U. Jepsen, M. Schall, V. Schyja, and H. Helm, Electro-optic detection of THz radiation in $LiTaO_3$, $LiNbO_3$ and ZnTe, Appl. Phys. Lett. **70**, 3069 (1997).

[39] G. Gallot and D. Grischkowsky, Electro-optic detection of terahertz radiation, J. Opt. Soc. Am. B **16**, 1204 (1999).

[40] S. Casalbuoni, H. Schlarb, B. Schmidt, P. Schmüser, B. Steffen, and A. Winter, Numerical studies on the electro-optic detection of femtosecond electron bunches, Phys. Rev. ST Accel. Beams **11**, 072802 (2008).

[41] N. Sei, H. Zen, and H. Ohgaki, Peak shift of coherent edge radiation spectrum depending on radio frequency field phase of accelerator, Appl. Sci. **12**, 626 (2022).